Loss of functional farnesoid X receptor increases atherosclerotic lesions in apolipoprotein E-deficient mice

Elyisha A. Hanniman,* Gilles Lambert,[†] Tanya C. McCarthy,* and Christopher J. Sinal[1,]*

Department of Pharmacology,* Dalhousie University, Halifax, Nova Scotia, Canada; and University of Nantes Medical School,[†] Institut National de la Santé et de la Recherche Médicale U539, Nantes, France

Abstract The farnesoid X receptor (FXR) is a bile acid-activated transcription factor that regulates the expression of genes critical for bile acid and lipid homeostasis. This study was undertaken to investigate the pathological consequences of the loss of FXR function on the risk and severity of atherosclerosis. For this purpose, FXR-deficient ($FXR^{-/-}$) mice were crossed with apolipoprotein E-deficient ($ApoE^{-/-}$) mice to generate $FXR^{-/-}ApoE^{-/-}$ mice. Challenging these mice with a high-fat, high-cholesterol (HF/HC) diet resulted in reduced weight gain and decreased survival compared with wild-type, $FXR^{-/-}$, and $ApoE^{-/-}$ mice. $FXR^{-/-}ApoE^{-/-}$ mice also had the highest total plasma lipids and the most atherogenic lipoprotein profile. Livers from $FXR^{-/-}$ and $FXR^{-/-}ApoE^{-/-}$ mice exhibited marked lipid accumulation, focal necrosis (accompanied by increased levels of plasma aspartate aminotransferase), and increased inflammatory gene expression. Measurement of en face lesion area of HF/HC-challenged mice revealed that although $FXR^{-/-}$ mice did not develop atherosclerosis, $FXR^{-/-}ApoE^{-/-}$ mice had approximately double the lesion area compared with $ApoE^{-/-}$ mice. In conclusion, loss of FXR function is associated with decreased survival, increased severity of defects in lipid metabolism, and more extensive aortic plaque formation in a mouse model of atherosclerotic disease.—Hanniman, E. A., G. Lambert, T. C. McCarthy, and C. J. Sinal. **Loss of functional farnesoid X receptor increases atherosclerotic lesions in apolipoprotein E-deficient mice.** *J. Lipid Res.* **2005.** 46: 2595–2604.

Supplementary key words atherosclerosis • nuclear receptor • liver

Dyslipidemia, characterized by low levels of HDL and high levels of LDL, is a known risk factor for the development of atherosclerosis. An important early event in this disease process is the deposition of lipid-filled plaques in the walls of arteries. Plaque formation is initiated when arterial wall macrophages accumulate modified LDL and initiate a chronic inflammatory state. Over time, this inflammatory state can lead to thickening of the arterial wall, fibrosis, and eventually rupture of the plaque, thrombosis, and occlusion of normal blood flow (1). The current regimen of pharmacological therapies for the treatment of cardiovascular disease remains incomplete, despite the fact that cardiovascular disease (characterized by atherosclerosis) remains the leading cause of death in Western societies (2, 3). Nuclear receptors are ligand-activated transcription factors that regulate many physiological and developmental processes, such as reproduction, metabolism, and cellular differentiation. This function is achieved by modulating the expression of target genes through binding to specific response elements in the promoter regions of these genes, leading to the recruitment of coactivators or corepressors that induce or repress the target gene, respectively (4). A number of nuclear receptors, including the liver X receptors and peroxisome proliferator-activated receptors, have important regulatory roles in lipid homeostasis (5–8). Consequently, a great deal of research has been devoted to the selective modulation of these receptors as a novel therapeutic approach to the prevention and treatment of atherosclerosis (9–11).

Excess cholesterol is transported from peripheral tissues to the liver by HDL-mediated reverse cholesterol transport (RCT). Once in the liver, cholesterol can be secreted into the bile either directly or after conversion to bile acids. The farnesoid X receptor (FXR) is a nuclear receptor that is activated by binding to bile acids and functions primarily as a bile acid sensor in the liver to induce and repress genes involved in bile acid export (bile salt export pump) and synthesis (cytochrome P450 7A1), respectively (12, 13). This conversion of cholesterol to bile acids and subsequent efflux to the bile is a quantitatively important contributor to RCT and by extension is also important for the prevention of atherosclerosis. Beyond this function, accumulating evidence strongly supports an expanded role for FXR in the regulation of systemic lipid

---

Abbreviations: apoC-II, apolipoprotein C-II; AST, aspartate aminotransferase; FPLC, fast-performance liquid chromatography; FXR, farnesoid X receptor; H+E, hematoxylin and eosin; HF/HC, high-fat/high-cholesterol; MAC1, macrophage antigen 1; RCT, reverse cholesterol transport; TNF-α, tumor necrosis factor-α.

[1] To whom correspondence should be addressed.
  e-mail: csinal@dal.ca

homeostasis. For example, FXR activates the expression of the genes encoding apolipoprotein C-II (apoC-II) and the LDL receptor (14, 15) and represses the expression of the genes encoding apoA-I and apoC-III as well as hepatic lipase (16, 17). More recently, FXR has also been linked to the regulation of carbohydrate metabolism (18–20). Together, these data indicate a broad regulatory role for FXR in systemic energy metabolism.

Given that FXR activation is linked to the repression of hepatic bile acid synthesis, agonists of this receptor would be expected to impair RCT and hepatic cholesterol elimination. Consistent with this, treatment of wild-type but not $FXR^{-/-}$ mice with the FXR antagonist guggulsterone has been reported to decrease hepatic cholesterol (21, 22). Paradoxically, $FXR^{-/-}$ mice exhibit increased blood triglyceride and cholesterol levels as well as increased accumulation of lipids in the liver, despite increased secretion of both bile acids and cholesterol (23, 24). Furthermore, FXR agonists have been shown to produce a potentially beneficial reduction of blood triglyceride in rodents (14, 17, 25). This study was undertaken to examine and clarify the pathological consequences of the loss of FXR function on lipid homeostasis and atherosclerotic progression. The results of this study indicate that targeted disruption of the FXR gene leads to more severe atherosclerosis in an established murine model of this disease and provide the first direct evidence linking this receptor to the risk and severity of cardiovascular disease.

MATERIALS AND METHODS

Animals and diets

$ApoE^{-/-}$ mice were purchased from Jackson Laboratories (Bar Harbor, ME). $FXR^{-/-}$ mice (from our breeding colony, backcrossed 10 generations to congenic C57BL/6J mice) were crossed with $ApoE^{-/-}$ mice to obtain the $FXR^{-/-}ApoE^{-/-}$ mice. The background of all mice used in this study was C57BL/6J. Seven- to 8-week-old male mice were placed on either chow (7% fat) (F4516; based on the AIN-93G diet) or a high-fat, high-cholesterol (HF/HC) diet containing 16% fat and 1.25% cholesterol (F4515; Bioserv, Frenchtown, NJ) for 12 weeks. Animals were weighed once per week, and food consumption was monitored throughout the study. All animals were housed at room temperature on a 12 h light/dark cycle and provided food and water ad libitum. All procedures were conducted at the Carleton Animal Care Facility in accordance with Canadian Council on Animal Care guidelines.

Plasma analyses

Blood was collected using heparinized needles after a 6 h fast and centrifuged at 6,700 g for 5 min. Plasma was stored at $-20°C$. Triglyceride and cholesterol levels were measured at 510 and 500 nm, respectively, using in vitro diagnostic reagents and calibrators (Thermo DMA, Arlington, TX) according to the manufacturer's instructions. Aspartate aminotransferase (AST) values were measured after dilution of the plasma 1:5 with distilled water and using an Infinity AST Reagent kit (Sigma Diagnostics, St. Louis, MO). Values were determined kinetically by the change in absorbance at 340 nm and at a temperature of 37°C. All absorbance measurements were performed using a 96-well plate reader (PowerWaveX; Bio-Tek Instruments, Inc., Winooski, VT). Blood glucose

was measured using a personal glucose monitoring device (TheraSense FreeStyle; AR-Med, Ltd.).

Fast-performance liquid chromatography and Western blot analysis

Fast-performance liquid chromatography (FPLC) separation of plasma lipoproteins from pooled plasma samples (200 µl; n = 3–5) and analysis of lipid content of the subsequent fractions were performed as described previously (26). Immunoblot analyses of apoB-100, apoB-48, apoA-I, and apoA-II in the VLDL, LDL, and HDL fractions (eluting at 14, 20, and 29 ml, respectively) were performed as described previously (24).

Liver lipid measurement

Lipids were extracted from liver tissue based on published methods (27). Solvents were evaporated from the extracted lipids under nitrogen and dissolved in Triton X-100 (Sigma-Aldrich, St. Louis, MO), warmed to 37°C, and mixed with water (1:4). The samples were then analyzed for triglyceride and cholesterol content using the same reagents (1 µl of sample:100 µl of reagent) listed above for plasma lipid analysis.

Histology

After 12 weeks on the diets, the largest lobe of the liver and the top half of the heart were obtained from the mice and embedded in OCT (Sakura Finetek U.S.A., Inc., Torrance, CA) combined with sucrose (20%) and stored at $-80°C$. Ten micrometer cryosections were obtained lengthwise through the liver lobe and 5 µm cryosections were obtained in cross-section through the aorta at the origin in the heart. All cryosections were fixed for 1 min in formaldehyde solution, stained for 10 min with Oil Red O (stains lipids red), and counterstained for 1 min with hematoxylin (stains nuclei blue) for qualitative observation of lipid accumulation. Five micrometer thick cross-sections were obtained from paraffin-embedded liver and stained with hematoxylin and eosin (H+E). En face lipid accumulation was determined by removing the aortas from the mice from the ileal bifurcation to the origin at the heart. The heart and the aorta were fixed for a minimum of 2 days in 5% neutral buffered formalin (EM Industries, Inc., Gibbstown, NJ) and 0.5× phosphate-buffered saline. The aortas were then cut longitudinally, splayed and pinned in a dish that was flooded with Sudan IV stain (stains lipids red) for 8 min, destained in 80% ethanol for 5 min, and photographed. Quantitation of plaques from the ileal bifurcation to the origin (not including any branching vessels) was performed using freehand selection of plaques using ImageJ software (National Institutes of Health, Bethesda, MD). The additive area of all the plaques in a given aorta was calculated as a percentage of the total surface area of the aorta.

Hepatic gene expression

Total hepatic RNA was isolated using Trizol reagent according to the supplier's instructions (Invitrogen, Carlsbad, CA). Quantitative RT-PCR analysis was performed as described previously (28) with the following modifications. Total RNA (2 µg) was reverse-transcribed using Stratascript reverse transcriptase (Stratagene, La Jolla, CA) with random hexamers pd(N)$_6$ according to the supplier's instructions. The synthesized cDNA was then amplified by quantitative PCR using a Stratagene MX3000p thermocycler in a total volume of 25 µl with Brilliant SYBR Green QPCR Master Mix. Primer sequences are as follows: murine tumor necrosis factor-α (TNF-α), 5′-CCC TCA CAC TCA GAT CAT CTT CT-3′ (forward) and 5′-GCT ACG ACG TGG GCT ACA G-3′ (reverse) (accession number NM_013693); murine macrophage antigen 1 (MAC1), 5′-GTG GTG CAG CTC ATC AAG AA-3′ (forward) and 5′-GCC ATG ACC TTT ACC TGG AA-3′ (reverse) (ac-

cession number M31039); and murine RNA polymerase II, 5′-CTG GAC CTA CCG GCA TGT TC-3′ (forward) and 5′-GTC ATC CCG CTC CCA ACA C-3′ (reverse) (accession number U37500). Thermal cycling conditions were identical for each primer pair and were as follows: a single cycle of 94°C for 10 min, followed by 40 cycles of denaturation at 94°C for 30 s, annealing at 60°C for 18 s, and elongation at 72°C for 30 s. Melting curves were generated from 60°C to 94°C at the end of the PCR protocol to ensure the amplification of a single product. The PCR products were then separated on a 2.5% agarose gel and visualized by ethidium bromide staining to ensure that a single product at the appropriate size was generated. Relative threshold cycle (C_T) values were obtained by the $\Delta\Delta C_T$ method (29) using a threshold of 10 standard deviations above background for C_T.

Statistics

All comparisons were performed within diet groups using one-way ANOVA with Tukey-Kramer postanalysis, unless stated otherwise. GraphPad Instat (Instat3 version 3.0a; GraphPad Software, Inc.) was used for all statistical analyses. Values are expressed as means ± SD. Differences between groups are considered statistically significant at $P \leq 0.05$.

RESULTS

$FXR^{-/-}ApoE^{-/-}$ mice have a decreased survival rate and fail to gain weight on a HF/HC diet

To study the effect that deletion of FXR has on atherosclerotic disease, $FXR^{-/-}$ mice were crossed with $ApoE^{-/-}$ mice to generate $FXR^{-/-}ApoE^{-/-}$ animals. Before crossing with the $ApoE^{-/-}$ mice (pure C57BL/6J background), the existing $FXR^{-/-}$ mouse model (24) was backcrossed 10 generations to a congenic C57BL/6J background. We then fed these mice standard rodent chow or the HF/HC diet containing increased levels of fat (16%, w/w) and cholesterol (1.25%, w/w) for a total of 12 weeks. Cholic acid is commonly included in atherogenic diets to increase the dietary absorption of lipids and to increase the inflammatory response. Because we have shown previously that dietary cholic acid is extremely toxic to $FXR^{-/-}$ mice (24), we omitted this component from our atherogenic diet. As

indicators of the general health of mice throughout the 12 week feeding study, starting weights (day 1), cumulative weight gain, food consumption, and survival rates were monitored. Starting weights were similar in all experimental groups with the exception of $FXR^{-/-}ApoE^{-/-}$ mice in the chow-fed group, which were of lower starting weight than $ApoE^{-/-}$ mice on the same diet (**Table 1**). $FXR^{-/-}ApoE^{-/-}$ mice on a HF/HC diet failed to gain weight to a similar magnitude as wild-type, $ApoE^{-/-}$, and $FXR^{-/-}$ mice on the same diet. $FXR^{-/-}ApoE^{-/-}$ mice on the HF/HC diet gained ∼2.8-fold less weight than $FXR^{-/-}$ and $ApoE^{-/-}$ mice and 3.7-fold less than wild-type mice on the same diet (Table 1). The reduced weight gain exhibited by $FXR^{-/-}ApoE^{-/-}$ mice was not attributable to reduced caloric intake, because the food consumption of this group did not differ from that of wild-type or $FXR^{-/-}$ mice (Table 1). $ApoE^{-/-}$ mice fed a HF/HC diet had the highest food consumption, consuming ∼1.3-fold more than the other groups on the same diet. Survival rates of the four genotypes of mice on both chow and the HF/HC diet were 100% with the exception of the $FXR^{-/-}ApoE^{-/-}$ mice on the HF/HC diet, which exhibited 66.7% survival (Table 1).

$FXR^{-/-}ApoE^{-/-}$ mice have increased blood levels of cholesterol, triglyceride, and AST

After 12 weeks on regular chow, blood cholesterol levels of $ApoE^{-/-}$ and $FXR^{-/-}ApoE^{-/-}$ mice were significantly greater than those of wild-type or $FXR^{-/-}$ mice fed the same diet but did not differ significantly from one another. $FXR^{-/-}ApoE^{-/-}$ mice challenged by a HF/HC diet had significantly greater cholesterol levels than all other genotypes on the same diet, with blood concentrations ∼11-, 6-, and 2-fold greater than those of wild-type, $FXR^{-/-}$, and $ApoE^{-/-}$ mice, respectively (Table 1). After 12 weeks on chow, triglyceride levels in both $FXR^{-/-}$ and $ApoE^{-/-}$ mice were ∼2-fold greater than those of wild-type mice on the same diet. $FXR^{-/-}ApoE^{-/-}$ triglyceride levels remained significantly higher than those of the other genotypes on the same diet, with blood concentrations ∼5-, 2-, and 2-fold

TABLE 1. Reduced survival and increased plasma lipids in $FXR^{-/-}ApoE^{-/-}$ mice

Diet	Initial Body Weight	Cumulative Weight Gain	Food Consumption	Survival	Plasma Cholesterol	Plasma Triglycerides	Plasma Aspartate Aminotransferase	Blood Glucose
	g		g/week	%	mg/dl		U/l	mmol/l
Chow								
Wild type	22.0 ± 1.0	5.4 ± 1.4	19.6 ± 0.7	100	69 ± 23	30 ± 10	35 ± 14	10.2 ± 1.5
$FXR^{-/-}$	21.2 ± 1.9	5.4 ± 1.3	20.0 ± 1.9	100	139 ± 30[a]	57 ± 6[a]	86 ± 43	11.8 ± 2.3
$ApoE^{-/-}$	24.3 ± 1.5	5.4 ± 2.0	22.9 ± 1.3	100	369 ± 80[a,b]	63 ± 16[a]	40 ± 23	11.7 ± 2.6
$FXR^{-/-}ApoE^{-/-}$	20.1 ± 2.9[c]	5.9 ± 1.8	20.4 ± 1.2	100	406 ± 124[a,b]	149 ± 14[a,b,c]	146 ± 49[a,c]	9.9 ± 1.2
High-fat/high-cholesterol								
Wild type	22.9 ± 1.1	8.6 ± 2.7	21.3 ± 2.7	100	96 ± 22	35 ± 9	51 ± 19	10.1 ± 1.7
$FXR^{-/-}$	24.2 ± 1.2	6.2 ± 2.0	18.8 ± 1.3	100	175 ± 28[a]	108 ± 40[a]	219 ± 49[a]	10.8 ± 1.2
$ApoE^{-/-}$	23.7 ± 1.6	6.6 ± 1.6	27.0 ± 0.9[a,b]	100	675 ± 178[a,b]	62 ± 24	92 ± 28[b]	10.7 ± 2.1
$FXR^{-/-}ApoE^{-/-}$	21.9 ± 1.3	2.3 ± 0.9[a,b,c]	20.4 ± 1.4[c]	66.7	1,017 ± 146[a,b,c]	129 ± 41[a,c]	349 ± 151[a,c]	13.8 ± 1.4

$ApoE^{-/-}$, apolipoprotein E-deficient; $FXR^{-/-}$, farnesoid X receptor-deficient. Values are given as means ± SD, n = 5–8. Statistical analyses were performed by one-way ANOVA within each diet group.
[a] $P < 0.05$ versus wild type.
[b] $P < 0.05$ versus $FXR^{-/-}$.
[c] $P < 0.05$ versus $ApoE^{-/-}$.

greater than in wild-type, $FXR^{-/-}$, and $ApoE^{-/-}$ mice, respectively (Table 1).

After 12 weeks on a HF/HC diet, blood levels of triglycerides in both $FXR^{-/-}$ and $FXR^{-/-}ApoE^{-/-}$ mice were ~3- and 2-fold greater than in wild-type and $ApoE^{-/-}$ mice, respectively. Plasma AST levels for chow-fed $FXR^{-/-}ApoE^{-/-}$ mice were ~4-fold greater compared with those in wild-type and $ApoE^{-/-}$ mice fed the same diet (Table 1). $FXR^{-/-}ApoE^{-/-}$ mice also had significantly greater plasma AST levels compared with chow-fed $FXR^{-/-}$ mice. HF/HC feeding led to a general increase of plasma AST levels in all of the genotypes studied. Similar to the chow-fed animals, the greatest plasma AST levels measured were those of $FXR^{-/-}$ and $FXR^{-/-}ApoE^{-/-}$ mice. Blood glucose levels did not differ significantly between groups at week 12 of the feeding study (Table 1).

$FXR^{-/-}ApoE^{-/-}$ mice have a more severe proatherogenic plasma lipoprotein profile

Further characterization of alterations in blood lipids caused by the deletion of FXR in the $ApoE^{-/-}$ mouse involved analysis of the lipoprotein profiles of these mice by FPLC (**Fig. 1**). Fractions obtained at elution volumes of 14, 20, and 29 ml (corresponding to the VLDL, LDL, and $HDL_{2/3}$ peaks, respectively) were further characterized by immunoblotting for apolipoprotein content (Fig. 1A, B, insets). On either chow or the HF/HC diet, $FXR^{-/-}$ mice had increased VLDL and LDL lipids as well as reduced $HDL_{2/3}$ cholesterol, apoA-I, and apoA-II compared with controls. The HDL peak was shifted toward smaller elution volumes (26–28 ml), indicating the presence of large triglyceride-rich HDL_1 particles only in the HF/HC-fed $FXR^{-/-}$ mice (Fig. 1A, C). In the $ApoE^{-/-}$ background, FXR deficiency increased the levels of VLDL apoB-48 and decreased those of HDL apoA-I and apoA-II. This was exacerbated by HF/HC feeding, with dramatically increased apoB-48 associated with VLDL and LDL as well as decreased apoA-I and apoA-II associated with HDL (Fig. 1B, inset) in $FXR^{-/-}ApoE^{-/-}$ mice.

Examination of the lipoprotein distribution patterns for cholesterol in the plasma of chow-fed $FXR^{-/-}ApoE^{-/-}$ and $ApoE^{-/-}$ mice revealed that $FXR^{-/-}ApoE^{-/-}$ mice had the highest amount of cholesterol in the VLDL fractions. HF/HC feeding of $FXR^{-/-}ApoE^{-/-}$ and $ApoE^{-/-}$ mice fur-
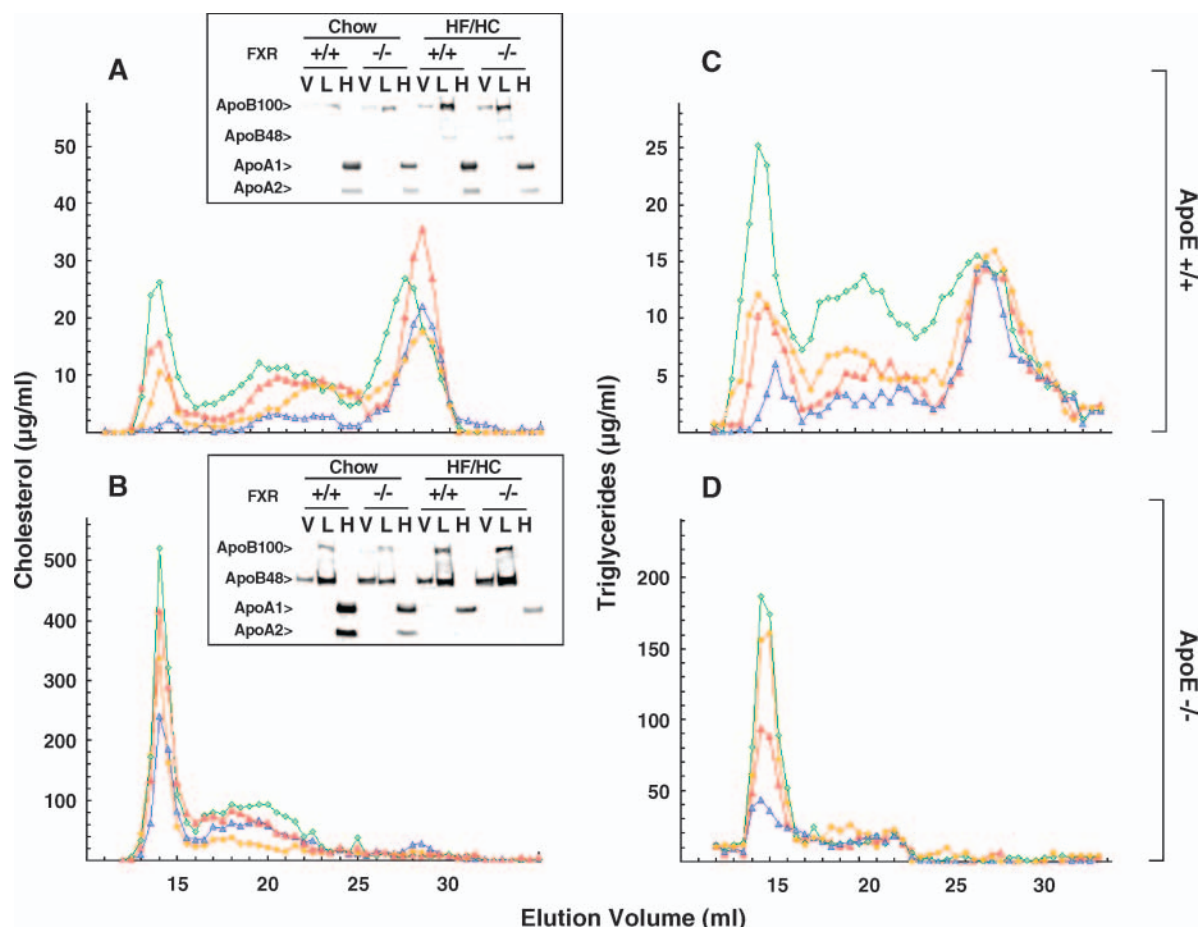

Fig. 1. Fast-performance liquid chromatography (FPLC) and Western blot analysis of plasma lipoprotein and apolipoprotein content. FPLC cholesterol (A) and triglyceride (C) profiles of wild-type mice fed chow (blue) or a high-fat/high-cholesterol (HF/HC; red) diet and of farnesoid X receptor-deficient ($FXR^{-/-}$) mice fed chow (yellow) or HF/HC (green). FPLC cholesterol (B) and triglyceride (D) profiles of apolipoprotein E-deficient ($ApoE^{-/-}$) mice fed chow (blue) or HF/HC (red) and of $ApoE^{-/-}FXR^{-/-}$ mice fed chow (yellow) or HF/HC (green). The insets show apolipoprotein Western blot analyses performed on fractions obtained from FPLC: V, VLDL; L, LDL; H, HDL. Serum (200 μl) was pooled from three to five animals for each experimental group.

ther increased plasma cholesterol in the form of VLDL in both genotypes. The levels of VLDL and LDL cholesterol were highest in $FXR^{-/-}ApoE^{-/-}$ mice compared with the other genotypes (Fig. 1B). In addition, $FXR^{-/-}ApoE^{-/-}$ animals had sharply increased VLDL triglyceride levels compared with $ApoE^{-/-}$ animals on both diets. Surprisingly, plasma triglycerides, eluting mostly in the VLDL range, were maximal in $FXR^{-/-}ApoE^{-/-}$ mice on both chow and the HF/HC diet (Fig. 1D).

$FXR^{-/-}ApoE^{-/-}$ mice challenged with a HF/HC diet exhibit hepatic lipid accumulation, focal necrosis, and inflammation

Given the importance of the liver in lipid homeostasis and RCT, liver histology (H+E examination for necrosis) in HF/HC-fed groups in addition to levels of triglyceride and cholesterol (in both chow- and HF/HC-fed mice) were examined. H+E staining of liver from HF/HC-fed mice revealed that both $FXR^{-/-}$ and $FXR^{-/-}ApoE^{-/-}$ mice had areas of focal necrosis, as indicated by localized accumulation of cells (most likely neutrophils and/or activated lymphocytes; **Fig. 2A**, arrowheads) (30). Similar indications of necrosis were not evident in the livers from HF/HC-fed wild-type and $ApoE^{-/-}$ mice. A qualitative approach to examine the hepatic accumulation of lipid was used by staining 10 μm sections of liver with Oil Red O (stains lipids red; Fig. 2A). Livers from $FXR^{-/-}$ and $FXR^{-/-}ApoE^{-/-}$ mice have increased lipid accumulation on a HF/HC diet compared with wild-type and $ApoE^{-/-}$ mice on the same diet (seen as large red vacuoles present in liver sections).

Lipids were organically extracted from liver tissue and measured using commercial colorimetric kits for both cholesterol and triglycerides. Interestingly, HF/HC feeding of $FXR^{-/-}$ and $FXR^{-/-}ApoE^{-/-}$ mice led to 4-fold increases in hepatic cholesterol over chow-fed mice of the same genotype compared with only 2- and 1.6-fold increases in wild-type and $ApoE^{-/-}$ mice, respectively (Fig. 2C). After 12 weeks on a HF/HC diet, $FXR^{-/-}$ and $FXR^{-/-}ApoE^{-/-}$ mice had increased hepatic concentrations of cholesterol, with increases of ~2-fold over both HF/HC-fed wild-type and $ApoE^{-/-}$ mice (Fig. 2C). HF/HC feeding increased hepatic triglycerides in $FXR^{-/-}$ mice (5-fold), $FXR^{-/-}ApoE^{-/-}$ mice (3-fold), and wild-type mice (2-fold) compared with the respective chow-fed controls (Fig. 2D). Similarly, both $FXR^{-/-}$ and $FXR^{-/-}ApoE^{-/-}$ mice fed the HF/HC diet had increased levels of hepatic triglycerides compared with wild-type and $ApoE^{-/-}$ groups on the same diet. Hepatic triglyceride concentrations in the $FXR^{-/-}$ mice were 2- and 3-fold greater than those of wild-type and $ApoE^{-/-}$ animals on the same diet, respectively (Fig. 2D). In accordance with the increased hepatic lipid accumulation, the liver weights (as a percentage of body weight) were increased for both HF/HC-fed $FXR^{-/-}$ and $FXR^{-/-}ApoE^{-/-}$ mice (5.4 ± 0.6 and 5.5 ± 0.6, respectively) compared with wild-type (3.9 ± 0.5) and $ApoE^{-/-}$ (4.3 ± 0.4) (Fig. 2E) mice fed the same diet.

In addition to histological and lipid analyses of livers from these mice, expression of the genes for TNF-α and MAC1 (markers of inflammation) was examined using real-time quantitative PCR. Chow-fed $FXR^{-/-}$, $ApoE^{-/-}$, and $FXR^{-/-}ApoE^{-/-}$ mice had ~3- to 4-fold higher levels of TNF-α expression compared with wild-type mice fed the same diet (Fig. 2F). HF/HC feeding dramatically increased TNF-α mRNA levels in both $FXR^{-/-}$ and $ApoE^{-/-}$ mice to ~10-fold over chow-fed wild-type mice. $FXR^{-/-}ApoE^{-/-}$ mice exhibited a synergistic increase in TNF-α gene expression to ~40-fold over wild-type values (Fig. 2F). Similar to the TNF-α expression patterns, both $FXR^{-/-}$ and $ApoE^{-/-}$ mice fed chow had similar mRNA expression (~5-fold over wild-type values) of hepatic MAC1 (Fig. 2G). Chow-fed $FXR^{-/-}ApoE^{-/-}$ mice had ~12-fold higher expression than wild-type mice on the same diet. HF/HC feeding led to increases in MAC1 mRNA levels (~15- to 17-fold over chow-fed wild-type mice) in both $FXR^{-/-}$ and $ApoE^{-/-}$ mice. Similar to TNF-α expression, MAC1 transcript levels showed a synergistic increase in HF/HC-fed $FXR^{-/-}ApoE^{-/-}$ mice (~68-fold higher than in the wild type).

Deletion of FXR results in more severe atherosclerosis in $ApoE^{-/-}$ mice

Determination of atherosclerosis was performed using cross-sectional as well as en face representations of aortas (stained for lipid-filled plaques) from all animals on both chow and the HF/HC diet (**Fig. 3**). Examination of both en face and cross-sectional aortas from the chow-fed mice revealed that neither wild-type nor $FXR^{-/-}$ animals had any detectable plaques on this diet (Fig. 3A, B). Both $FXR^{-/-}ApoE^{-/-}$ and $ApoE^{-/-}$ mice fed chow had small amounts of detectable plaques in both cross-sectional and en face representations (Fig. 3A, B). The extent of atherosclerosis in aortas from these chow-fed $ApoE^{-/-}FXR^{-/-}$ and $ApoE^{-/-}$ mice, as determined by quantitation of en face plaques, was not significantly different (**Fig. 4A**). Challenging both wild-type and $FXR^{-/-}$ mice with a HF/HC diet did not result in detectable atherosclerotic plaques, as indicated by cross-sectional or en face aortas from these mice (Fig. 3A, B). In contrast, HF/HC feeding of $ApoE^{-/-}$ and $FXR^{-/-}ApoE^{-/-}$ mice resulted in large increases in the extent of atherosclerosis in aortas of these mice (Fig. 3A, B). Quantitation of atherosclerosis in en face aortas from these mice revealed that the $FXR^{-/-}ApoE^{-/-}$ mice had approximately double the amount of plaques compared with the $ApoE^{-/-}$ mice (37.2 ± 11.4% relative to 18.2 ± 3.2%) (Fig. 4B).

DISCUSSION

This study investigated the pathological consequences of deficient FXR function for the development of atherosclerotic disease. Challenging mice that lacked both functional FXR and apoE genes with a HF/HC diet led to a failure to gain weight to a similar extent and decreased survival compared with wild-type, $FXR^{-/-}$, and $ApoE^{-/-}$ mice fed the same diet. Loss of functional FXR also led to further increases of total blood cholesterol and triglycer-
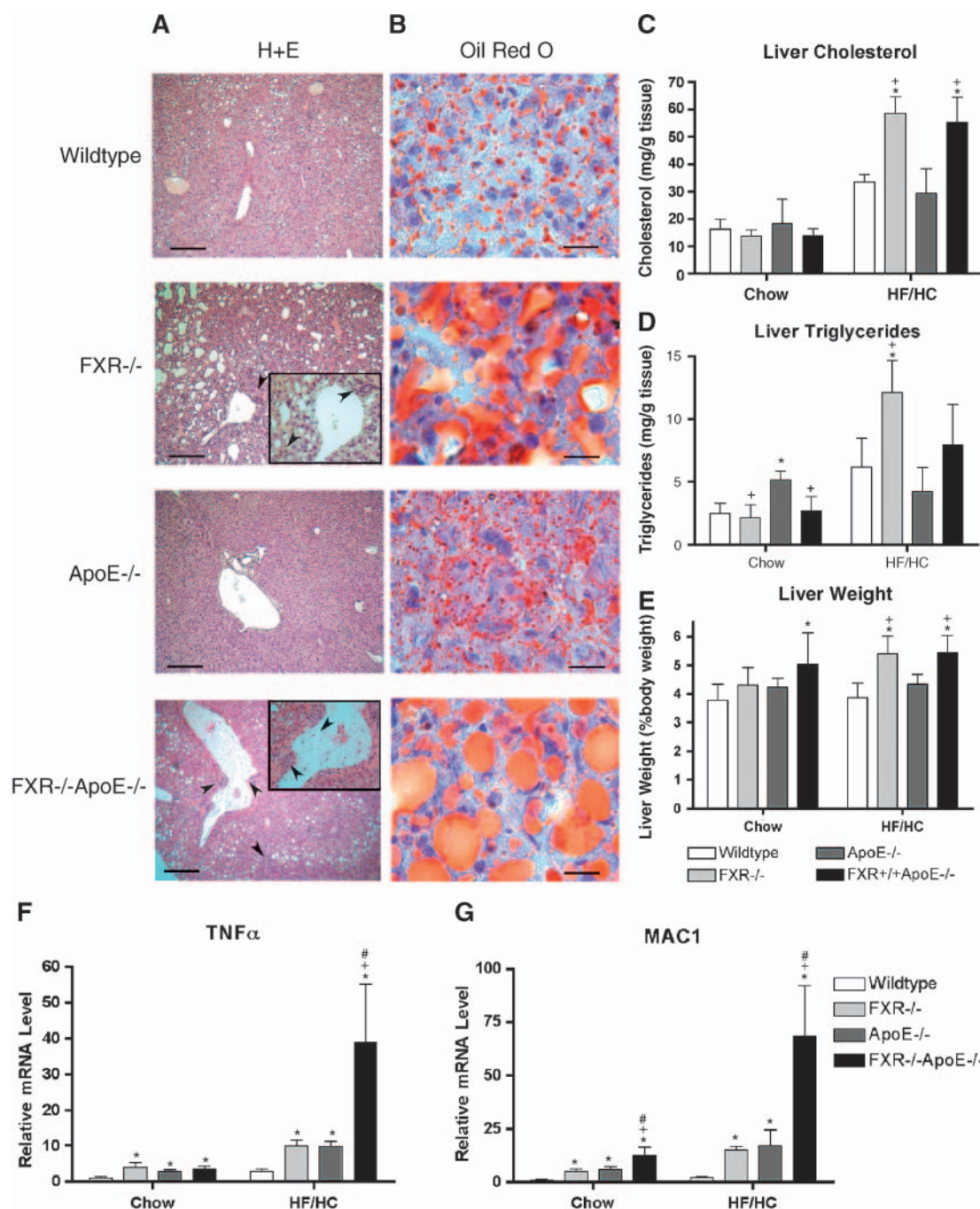
Fig. 2. Analyses of hepatic lipid accumulation, necrosis, and inflammation. A: Hematoxylin and eosin (H+E)-stained sections (5 μm) of liver from HF/HC-fed mice (100×). Insets are 400×. Arrowheads indicate the accumulation of immune cells. B: Oil Red O-stained sections (5 μm) of liver from HF/HC mice (1,000×). C: Total hepatic cholesterol. D: Triglyceride. E: Liver body weight. Real-time quantitative PCR analysis of hepatic tumor necrosis factor-α (TNF-α; F) and macrophage antigen 1 (MAC1; G) mRNA levels. All values shown are means ± SD and were normalized to RNA polymerase II mRNA levels; they are expressed as the fold difference relative to chow-fed wild-type mice. * $P <$ 0.05 versus wild-type mice, # $P < 0.05$ versus $FXR^{-/-}$ mice, and + $P < 0.05$ versus $ApoE^{-/-}$ mice on the same diet. n = 3 for hepatic lipids, n = 4–5 for real-time quantitative PCR. Bars = 50 μm.

ide levels as well as increased VLDL and LDL in the $ApoE^{-/-}$ model. HF/HC-fed $FXR^{-/-}ApoE^{-/-}$ mice experienced the greatest detrimental effects on hepatic status, as shown by massive lipid accumulation, focal necrosis, and markedly increased inflammatory gene expression and plasma AST levels. Ultimately, all of these phenotypic characteristics were associated with the most severe de-

gree of atherosclerotic lesion formation and the lowest survivability in the HF/HC-fed $FXR^{-/-}ApoE^{-/-}$ mice compared with the other genotypes studied.

Our previous work demonstrated decreased hepatic expression of the scavenger receptor class B type I in $FXR^{-/-}$ mice. This was associated with decreased hepatic uptake of HDL cholesterol as well as increased synthesis of highly
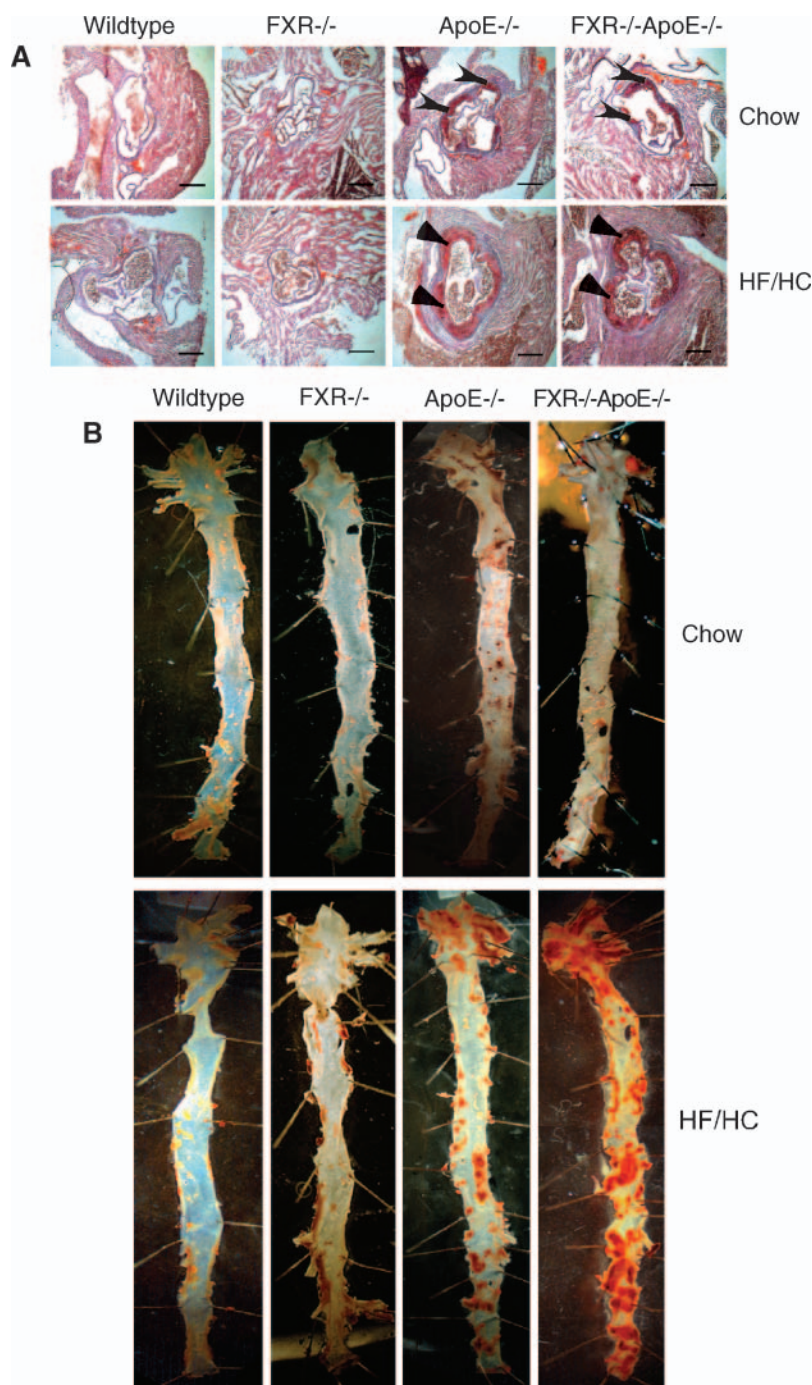
Fig. 3. Analysis of aortic atherosclerosis in chow- and HF/HC-fed mice. A: Oil Red O-stained cross-sections (5 μm) through aortic roots, 700 μm past the appearance of the aortic valve (1,000×). Bars = 50 μm. B: En face staining of Sudan IV-stained aortas. Arrowheads and wedges indicate atherosclerotic plaques in chow- and HF/HC-fed animals, respectively.

atherogenic apoB-containing lipoproteins (23). Additionally, $FXR^{-/-}$ mice exhibit hyperabsorption of cholesterol (23) and triglycerides (unpublished results) from the intestine. All of these factors are believed to contribute to the proatherogenic plasma total lipid and lipoprotein profile exhibited by $FXR^{-/-}$ mice. ApoE is required for hepatic LDL receptor-mediated clearance of remnants of VLDL in the liver (31), and consistent with previous studies (32, 33), we observed an almost complete absence of

HDL in the plasma of $ApoE^{-/-}$ mice. Thus, the extremely atherogenic plasma lipid and lipoprotein profile exhibited by $FXR^{-/-}ApoE^{-/-}$ mice, particularly when challenged with a HF/HC diet, reflects the striking genetic interaction between the loss of function of the FXR and apoE alleles.

Histological analysis of livers from HF/HC-fed mice revealed that both $FXR^{-/-}$ and $FXR^{-/-}ApoE^{-/-}$ mice had areas of focal necrosis that were absent from the livers of
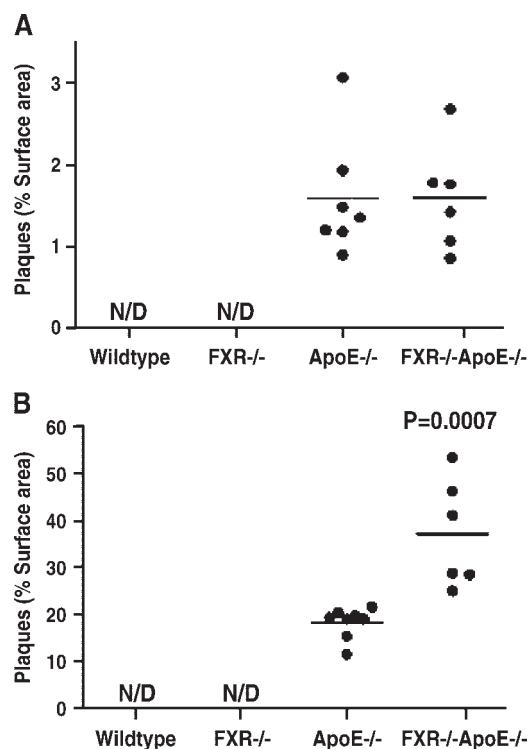
Fig. 4. Quantitation of aortic atherosclerosis in chow- and HF/HC-fed mice. A: Quantitation of atherosclerotic plaques in chow-fed mice (percentage total en face aorta surface area). B: Quantitation of atherosclerotic plaques in HF/HC-fed mice (percentage total en face aorta surface area). n = 5–8. $P = 0.0007$ compared with $ApoE^{-/-}$ mice on the HF/HC diet (Mann-Whitney U-test).

$ApoE^{-/-}$ and wild-type mice fed the same diet. Consistent with this observation, HF/HC-fed $FXR^{-/-}$ and $FXR^{-/-}ApoE^{-/-}$ mice also exhibited the highest levels of plasma AST, which may have resulted from the release of this enzyme from necrotic hepatocytes. Hepatic lipid accumulation is a hallmark feature of the pathogenesis of necrotic liver diseases such as nonalcoholic steatohepatitis (34). Thus, given the massive hepatic accumulation of lipid in both $FXR^{-/-}$ and $FXR^{-/-}ApoE^{-/-}$ mice, it is not surprising that chronic HF/HC feeding caused damage to the livers of these animals. Furthermore, $FXR^{-/-}$ mice present with a cholestatic phenotype characterized by increased plasma bile acids (24). This may have also contributed to the hepatic necrosis seen in $FXR^{-/-}$ and $FXR^{-/-}ApoE^{-/-}$ mice when fed a HF/HC diet. Indicators of an altered inflammatory state in the liver included changes in expression of the immune receptor MAC1 and the inflammatory cytokine TNF-α. MAC1, also known as CD11b/CD18 and complement receptor 3, is predominantly expressed on macrophages, monocytes, neutrophils, and natural killer cells and is involved in many functions, including activation and migration of these cells (35). TNF-α is a proinflammatory cytokine released by tissue macrophages and T-cells at a site of injury and essentially acts to activate and attract other immune cells (36). TNF-α has also been shown to induce the upregulation of MAC1 in neutrophils (37). Therefore, the dramatic increase of MAC1 and TNF-α

mRNA levels in the livers of HF/HC-fed $FXR^{-/-}ApoE^{-/-}$ mice most likely represented the combined effects of inflammation-induced expression of these genes in hepatocytes and infiltrating cells of the immune system such as macrophages and neutrophils. In addition, increased TNF-α levels in the $FXR^{-/-}ApoE^{-/-}$ mice may have added to the induction of MAC1 expression in these immune cells. Combined with the failure to gain as much body weight and reduced survival compared with the other genotypes, these data suggest that hepatic toxicity and severe dysfunction occurred in the HF/HC-challenged $FXR^{-/-}ApoE^{-/-}$ mice.

Although loss of FXR function alone was not sufficient to cause atherosclerosis when mice were challenged with a HF/HC diet, the combination of FXR deficiency with that of apoE resulted in a dramatic worsening of the disease. Unlike humans, mice transport the majority of plasma lipids in HDL particles, and this is thought to contribute to the inherent resistance of this species to atherosclerotic disease. Compared with wild-type animals, $FXR^{-/-}$ mice exhibit a proatherogenic plasma lipoprotein profile characterized by the presence of increased amounts of highly atherogenic VLDL and LDL particles in the plasma. Therefore, it was somewhat surprising that no atherosclerosis was detected in the $FXR^{-/-}$ mice fed the HF/HC diet. ApoE is synthesized in large quantities by the liver, is a constituent of all lipoproteins except LDL, and functions as a ligand for receptors that clear chylomicrons and VLDL remnants from the blood (32). ApoE is also synthesized by monocytes and macrophages and is thought to promote cholesterol efflux and modulate inflammatory responses in atherosclerotic vessels (33). Thus, the increased susceptibility of $ApoE^{-/-}$ mice to spontaneous and diet-induced atherosclerotic lesions results from a loss of critical functions in at least two sites, the liver and macrophage. In contrast, although FXR has well-defined regulatory roles in hepatic function, the expression of this receptor in macrophages is undetectable (unpublished results) (38). Thus, despite the severe proatherogenic plasma lipid profile of $FXR^{-/-}$ mice, it is likely that macrophages in the vessel walls of these mice remain resistant to lipid accumulation and plaque formation. Only when the loss of functional FXR was combined with the loss of apoE was a genetic interaction resulting in more severe dyslipidemia, impaired hepatic function, and atherosclerosis revealed.

Recently, treatment with the selective FXR agonist GW4064 was shown to prevent the development of gallstones in a mouse model of the disease (39). Importantly, this study demonstrated that modulation of FXR could be used to treat a specific disease process and more generally illustrated the therapeutic potential of targeting this receptor. At present, however, the benefits of manipulating FXR function as a novel therapeutic approach for atherosclerosis are not clear. Presumably, activation of FXR in vivo would lead to decreased conversion of cholesterol to bile acids, an effect detrimental to the treatment of coronary artery disease and hyperlipidemia. However, data generated in our study as well as previous

work with $FXR^{-/-}$ mice have demonstrated that the role of FXR in lipid homeostasis is more complicated than previously thought. For instance, $FXR^{-/-}$ mice exhibit increased intestinal absorption of cholesterol and triglycerides, decreased hepatic uptake of HDL, and increased synthesis of apoB-containing lipoproteins (23). All of these characteristics associated with the loss of FXR function suggest that antagonism of this receptor would lead to an undesirable disruption of systemic lipid homeostasis that ultimately may be detrimental to the treatment of atherosclerosis. In addition, it is not known whether modulation of hepatic FXR function can affect the inflammatory state at the level of the vessel wall in addition to that seen in the liver in this study. Studies of the lipid-lowering mechanism of an herbal product, guggulsterone, revealed antagonism of FXR and a decrease of hepatic cholesterol accumulation (21, 22) as well as hypolipidemic effects and increased hepatic LDL uptake (40). These findings lead to the question of why antagonism of FXR by guggulsterone is lipid-lowering but targeted disruption of the FXR gene leads to hyperlipidemia and increased atherosclerosis when combined with loss of apoE function. One answer to this controversy may be provided by recent work demonstrating that guggulsterone antagonizes a number of nuclear receptors (including glucocorticoid, mineralocorticoid, and androgen receptors) with up to 100-fold greater potency than that exhibited for FXR (41). Furthermore, guggulsterone is also a potent activator of a number of other nuclear receptors, including the estrogen, progesterone, and pregnane X receptors (42). Therefore, the in vivo effects of guggulsterone are likely to be mediated by several mechanisms other than antagonism of FXR.

In conclusion, this study demonstrates that loss of FXR function causes increased atherosclerosis in the $ApoE^{-/-}$ mouse model of this disease. Other outcomes precipitated by the loss of FXR in this model included decreased weight gain and survival, increased hepatic and plasma lipids, increased hepatic inflammation, and a more severe plasma lipoprotein profile. This study is the first to demonstrate a pathogenic role for FXR in atherosclerosis using an in vivo model of the disease. In contrast to other nuclear receptors with roles in macrophage lipid homeostasis (e.g., liver X receptors, peroxisome proliferator-activated receptors), the worsening of atherosclerosis caused by targeted deletion of FXR appears to be a consequence of the loss of function of this receptor in liver and gut only. Our data demonstrate the pathological consequences of a lack of FXR function and the potential for genetic interactions of deleterious mutations of the gene for this nuclear receptor with other gene mutations known to increase the risk for cardiovascular disease.

REFERENCES

1. Lusis, A. J. 2000. Atherosclerosis. *Nature.* **407:** 233–241.
2. Canada, S. 2002. Leading Causes of Death 2002. (Statistics Canada, Ottawa, Ontario).
3. Hoyert, D. L. H-C. Kung, and B. L. Smith. 2005. Deaths: preliminary data for 2003. *In* National Vital Statistics Reports. (National Center for Health Statistics, Hyattsville, MD) **53:** 1–23 .
4. Francis, G. A., E. Fayard, F. Picard, and J. Auwerx. 2003. Nuclear receptors and the control of metabolism. *Annu. Rev. Physiol.* **65:** 261–311.
5. Tontonoz, P., and D. J. Mangelsdorf. 2003. Liver X receptor signaling pathways in cardiovascular disease. *Mol. Endocrinol.* **17:** 985–993.
6. Lee, C. H., P. Olson, and R. M. Evans. 2003. Minireview. Lipid metabolism, metabolic diseases, and peroxisome proliferator-activated receptors. *Endocrinology.* **144:** 2201–2207.
7. Barish, G. D., and R. M. Evans. 2004. PPARs and LXRs: atherosclerosis goes nuclear. *Trends Endocrinol. Metab.* **15:** 158–165.
8. Chinetti-Gbaguidi, G., J. C. Fruchart, and B. Staels. 2005. Role of the PPAR family of nuclear receptors in the regulation of metabolic and cardiovascular homeostasis: new approaches to therapy. *Curr. Opin. Pharmacol.* **5:** 177–183.
9. Hanniman, E. A., and C. J. Sinal. 2004. Nuclear receptors: novel therapeutic targets for the treatment and prevention of atherosclerosis. *Drug Discovery Today: Therapeutic Strategies.* **1:** 155–161.
10. Castrillo, A., and P. Tontonoz. 2004. PPARs in atherosclerosis: the clot thickens. *J. Clin. Invest.* **114:** 1538–1540.
11. Berger, J. P., T. E. Akiyama, and P. T. Meinke. 2005. PPARs: therapeutic targets for metabolic disease. *Trends Pharmacol. Sci.* **26:** 244–251.
12. Goodwin, B., S. A. Jones, R. R. Price, M. A. Watson, D. D. McKee, L. B. Moore, C. Galardi, J. G. Wilson, M. C. Lewis, M. E. Roth, et al. 2000. A regulatory cascade of the nuclear receptors FXR, SHP-1, and LRH-1 represses bile acid biosynthesis. *Mol. Cell.* **6:** 517–526.
13. Schuetz, E. G., S. Strom, K. Yasuda, V. Lecureur, M. Assem, C. Brimer, J. Lamba, R. B. Kim, V. Ramachandran, B. J. Komoroski, et al. 2001. Disrupted bile acid homeostasis reveals an unexpected interaction among nuclear hormone receptors, transporters, and cytochrome P450. *J. Biol. Chem.* **276:** 39411–39418.
14. Kast, H. R., C. M. Nguyen, C. J. Sinal, S. A. Jones, B. A. Laffitte, K. Reue, F. J. Gonzalez, T. M. Willson, and P. A. Edwards. 2001. Farnesoid X-activated receptor induces apolipoprotein C-II transcription: a molecular mechanism linking plasma triglyceride levels to bile acids. *Mol. Endocrinol.* **15:** 1720–1728.
15. Sirvent, A., T. Claudel, G. Martin, J. Brozek, V. Kosykh, R. Darteil, D. W. Hum, J. C. Fruchart, and B. Staels. 2004. The farnesoid X receptor induces very low density lipoprotein receptor gene expression. *FEBS Lett.* **566:** 173–177.
16. Claudel, T., E. Sturm, H. Duez, I. P. Torra, A. Sirvent, V. Kosykh, J. C. Fruchart, J. Dallongeville, D. W. Hum, F. Kuipers, et al. 2002. Bile acid-activated nuclear receptor FXR suppresses apolipoprotein A-I transcription via a negative FXR response element. *J. Clin. Invest.* **109:** 961–971.
17. Claudel, T., Y. Inoue, O. Barbier, D. Duran-Sandoval, V. Kosykh, J. Fruchart, J. C. Fruchart, F. J. Gonzalez, and B. Staels. 2003. Farnesoid X receptor agonists suppress hepatic apolipoprotein CIII expression. *Gastroenterology.* **125:** 544–555.
18. Stayrook, K. R., K. S. Bramlett, R. S. Savkur, J. Ficorilli, T. Cook, M. E. Christe, L. F. Michael, and T. P. Burris. 2005. Regulation of carbohydrate metabolism by the farnesoid X receptor. *Endocrinology.* **146:** 984–991.
19. Duran-Sandoval, D., G. Mautino, G. Martin, F. Percevault, O. Barbier, J. C. Fruchart, F. Kuipers, and B. Staels. 2004. Glucose regulates the expression of the farnesoid X receptor in liver. *Diabetes.* **53:** 890–898.
20. Duran-Sandoval, D., B. Cariou, F. Percevault, N. Hennuyer, A. Grefhorst, T. H. van Dijk, F. J. Gonzalez, J. C. Fruchart, F. Kuipers, and B. Staels. 2005. The farnesoid X receptor modulates hepatic carbohydrate metabolism during the fasting-refeeding transition. *J. Biol. Chem.* **280:** 29971–29979.
21. Wu, J., C. Xia, J. Meier, S. Li, X. Hu, and D. S. Lala. 2002. The hypolipidemic natural product guggulsterone acts as an antagonist of the bile acid receptor. *Mol. Endocrinol.* **16:** 1590–1597.
22. Urizar, N. L., A. B. Liverman, D. T. Dodds, F. V. Silva, P. Ordentlich, Y. Yan, F. J. Gonzalez, R. A. Heyman, D. J. Mangelsdorf, and D. D.

Moore. 2002. A natural product that lowers cholesterol as an antagonist ligand for FXR. *Science.* **296:** 1703–1706.

23. Lambert, G., M. J. Amar, G. Guo, H. B. Brewer, Jr., F. J. Gonzalez, and C. J. Sinal. 2003. The farnesoid X-receptor is an essential regulator of cholesterol homeostasis. *J. Biol. Chem.* **278:** 2563–2570.

24. Sinal, C. J., M. Tohkin, M. Miyata, J. M. Ward, G. Lambert, and F. J. Gonzalez. 2000. Targeted disruption of the nuclear receptor FXR/BAR impairs bile acid and lipid homeostasis. *Cell.* **102:** 731–744.

25. Maloney, P. R., D. J. Parks, C. D. Haffner, A. M. Fivush, G. Chandra, K. D. Plunket, K. L. Creech, L. B. Moore, J. G. Wilson, M. C. Lewis, et al. 2000. Identification of a chemical tool for the orphan nuclear receptor FXR. *J. Med. Chem.* **43:** 2971–2974.

26. Lambert, G., M. J. Amar, P. Martin, J. Fruchart-Najib, B. Foger, R. D. Shamburek, H. B. Brewer, Jr., and S. Santamarina-Fojo. 2000. Hepatic lipase deficiency decreases the selective uptake of HDL-cholesteryl esters in vivo. *J. Lipid Res.* **41:** 667–672.

27. Carlson, S. E., and S. Goldfarb. 1977. A sensitive enzymatic method for determination of free and esterified tissue cholesterol. *Clin. Chim. Acta.* **79:** 575–582.

28. McCarthy, T. C., X. Li, and C. J. Sinal. 2005. Vitamin D receptor-dependent regulation of colon multidrug resistance-associated protein 3 gene expression by bile acids. *J. Biol. Chem.* **280:** 23232–23242.

29. Livak, K. J., and T. D. Schmittgen. 2001. Analysis of relative gene expression data using real-time quantitative PCR and the 2(-Delta Delta C(T)) method. *Methods.* **25:** 402–408.

30. Monshouwer, M., and K. H. Hoebe. 2003. Hepatic (dys-)function during inflammation. *Toxicol. In Vitro.* **17:** 681–686.

31. Linton, M. F., A. H. Hasty, V. R. Babaev, and S. Fazio. 1998. Hepatic apo E expression is required for remnant lipoprotein clearance in the absence of the low density lipoprotein receptor. *J. Clin. Invest.* **101:** 1726–1736.

32. Meir, K. S., and E. Leitersdorf. 2004. Atherosclerosis in the apolipoprotein-E-deficient mouse: a decade of progress. *Arterioscler. Thromb. Vasc. Biol.* **24:** 1006–1014.

33. Curtiss, L. K., and W. A. Boisvert. 2000. Apolipoprotein E and atherosclerosis. *Curr. Opin. Lipidol.* **11:** 243–251.

34. Wanless, I. R., and K. Shiota. 2004. The pathogenesis of nonalcoholic steatohepatitis and other fatty liver diseases: a four-step model including the role of lipid release and hepatic venular obstruction in the progression to cirrhosis. *Semin. Liver Dis.* **24:** 99–106.

35. Arnaout, M. A. 1990. Structure and function of the leukocyte adhesion molecules CD11/CD18. *Blood.* **75:** 1037–1050.

36. Varfolomeev, E. E., and A. Ashkenazi. 2004. Tumor necrosis factor: an apoptosis JuNKie? *Cell.* **116:** 491–497.

37. Witthaut, R., A. Farhood, C. W. Smith, and H. Jaeschke. 1994. Complement and tumor necrosis factor-alpha contribute to Mac-1 (CD11b/CD18) up-regulation and systemic neutrophil activation during endotoxemia in vivo. *J. Leukoc. Biol.* **55:** 105–111.

38. Perez, A., J. L. Thuillard, C. L. Bentzen, and E. J. Niesor. 2003. Expression of nuclear receptors and apo E secretion during the differentiation of monocytic THP-1 cells into macrophages. *Cell Biol. Toxicol.* **19:** 95–105.

39. Moschetta, A., A. L. Bookout, and D. J. Mangelsdorf. 2004. Prevention of cholesterol gallstone disease by FXR agonists in a mouse model. *Nat. Med.* **10:** 1352–1358.

40. Singh, V., S. Kaul, R. Chander, and N. K. Kapoor. 1990. Stimulation of low density lipoprotein receptor activity in liver membrane of guggulsterone treated rats. *Pharmacol. Res.* **22:** 37–44.

41. Burris, T. P., C. Montrose, K. A. Houck, H. E. Osborne, W. P. Bocchinfuso, B. C. Yaden, C. C. Cheng, R. W. Zink, R. J. Barr, C. D. Hepler, et al. 2005. The hypolipidemic natural product guggulsterone is a promiscuous steroid receptor ligand. *Mol. Pharmacol.* **67:** 948–954.

42. Brobst, D. E., X. Ding, K. L. Creech, B. Goodwin, B. Kelley, and J. L. Staudinger. 2004. Guggulsterone activates multiple nuclear receptors and induces CYP3A gene expression through the pregnane X receptor. *J. Pharmacol. Exp. Ther.* **310:** 528–535.